Geomorphology 138 (2012) 1–14

Contents lists available at SciVerse ScienceDirect

Geomorphology

journal homepage: www.elsevier.com/locate/geomorph

Assessment of pingo distribution and morphometry using an IfSAR derived digital surface model, western Arctic Coastal Plain, Northern Alaska

Benjamin M. Jones [a,b,*], Guido Grosse [b], Kenneth M. Hinkel [c], Christopher D. Arp [d], Shane Walker [e], Richard A. Beck [c], John P. Galloway [f]

[a] Alaska Science Center, U.S. Geological Survey, 4210 University Drive, Anchorage, AK 99508, USA
[b] Geophysical Institute, University of Alaska Fairbanks, 903 Koyukuk Drive, Fairbanks, AK 99775, USA
[c] Department of Geography, University of Cincinnati, 401 Braunstein Hall, Cincinnati, OH 45221, USA
[d] Water and Environmental Research Center, University of Alaska Fairbanks, 467 Duckering Building, Fairbanks, AK 99775, USA
[e] Arctic Field Office, Bureau of Land Management, 1150 University Avenue, Fairbanks, AK 99709, USA
[f] U.S. Geological Survey (Retired), 345 Middlefield Road, Menlo Park, CA 94025, USA

ARTICLE INFO

Article history:
Received 4 March 2011
Received in revised form 26 July 2011
Accepted 6 August 2011
Available online 16 August 2011

Keywords:
Drained lake basin
Ground ice
IfSAR
Periglacial landform
Permafrost
Pingo

ABSTRACT

Pingos are circular to elongate ice-cored mounds that form by injection and freezing of pressurized water in near-surface permafrost. Here we use a digital surface model (DSM) derived from an airborne Interferometric Synthetic Aperture Radar (IfSAR) system to assess the distribution and morphometry of pingos within a 40,000 km^2 area on the western Arctic Coastal Plain of northern Alaska. We have identified 1247 pingo forms in the study region, ranging in height from 2 to 21 m, with a mean height of 4.6 m. Pingos in this region are of hydrostatic origin, with 98% located within 995 drained lake basins, most of which are underlain by thick eolian sand deposits. The highest pingo density (0.18 km^{-2}) occurs where streams have reworked these deposits. Morphometric analyses indicate that most pingos are small to medium in size (<200 m diameter), gently to moderately sloping (<30°), circular to slightly elongate (mean circularity index of 0.88), and of relatively low height (2 to 5 m). However, 57 pingos stand higher than 10 m, 26 have a maximum slope greater than 30°, and 42 are larger than 200 m in diameter. Comparison with a legacy pingo dataset based on 1950s stereo-pair photography indicates that 66 may have partially or completely collapsed over the last half-century. However, we mapped over 400 pingos not identified in the legacy dataset, and identified only three higher than 2 m to have formed between ca. 1955 and ca. 2005, indicating that caution should be taken when comparing contemporary and legacy datasets derived by different techniques. This comprehensive database of pingo location and morphometry based on an IfSAR DSM may prove useful for land and resource managers as well as aid in the identification of pingo-like features on Mars.

Published by Elsevier B.V.

1. Introduction

A pingo is a type of "perennial frost mound consisting of a core of massive ice, produced primarily by injection of water, and covered with soil and vegetation" (van Everdingen, 1998). The name derives from an Inuit word meaning a conical hill and was introduced to the literature by Porsild (1929). Porsild (1938) later suggested the term pingo be used in a technical sense to refer to sizeable ice-cored mounds occurring in the Mackenzie Delta region, Canada. Since then this term has been widely adopted in the scientific literature. Synonymous Russian names include the Yakutian term *bulgunnyakh* and the terms *ledyanoy bugor* and *ledyanoy kholm* commonly used in western and northern Siberia (Grosse and Jones, 2011). Pingos are differentiated from other ice-cored mounds such as palsas, lithalsas, hydrolaccoliths, and broad-based mounds based largely upon formative process, internal structure of ice core, size, overburden, and environmental setting (Walker et al., 1985; Seppala, 1986; Worsley et al., 1995; Gurney, 2001; Pissart, 2002). Pingos are further differentiated from other similar, yet smaller seasonal and perennial ice-cored mounds, ranging from 5 to 20 m in diameter and up to 1 m tall (Muller, 1945; Nelson et al., 1992; Pollard and van Everdingen, 1992; Mackay, 1998).

Pingos provide a direct indication of the presence of permafrost. In general, pingos form by the injection and freezing of pressurized water in near-surface permafrost resulting in the formation of an ice core, with concurrent heave or updoming of the overlying sediments. This is due to the 9% volume increase upon phase shift from water to ice as well as continued injection of water and formation of a massive ice core. Two water pressure mechanisms are recognized: hydrostatic (closed-system) and hydraulic (open-system) (Müller, 1959; Mackay, 1979). Hydrostatic pingos commonly occur in regions underlain by continuous permafrost. They tend to form in drained lake basins that are underlain

* Corresponding author. Tel.: +1 907 786 7033.
E-mail address: bjones@usgs.gov (B.M. Jones).

0169-555X/$ – see front matter. Published by Elsevier B.V.
doi:10.1016/j.geomorph.2011.08.007

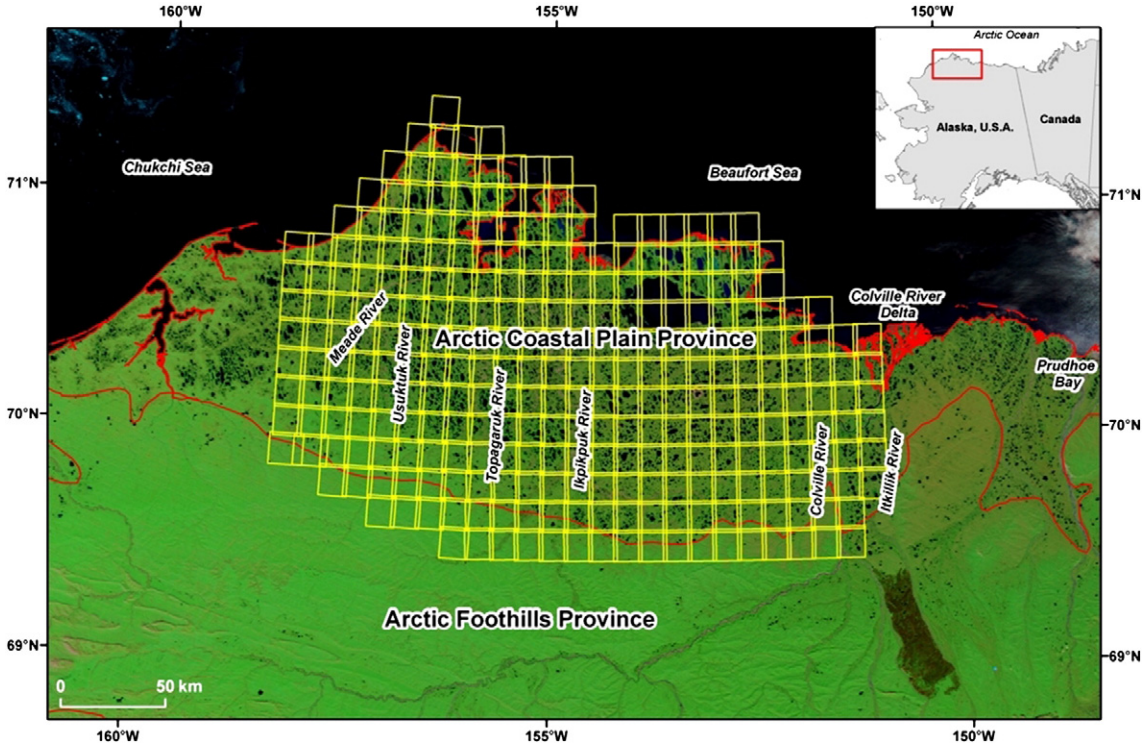

Fig. 1. MODIS image base map of a portion of northern Alaska. The yellow rectangles represent the 315 IfSAR DSM tiles used to assess the distribution and morphometry of pingos located on the western Arctic Coastal Plain. The southern margin of the red polygon demarcates the physiographic boundary between the Coastal Plain and Foothills Provinces.

by saturated sands, yet have a layer of finer material near the surface. They initiate through the expulsion of pore water caused by closed-system freezing of a talik in recently drained lake basins due to aggradation of permafrost from above and below (Mackay, 1979, 1998). In contrast, hydraulic pingos largely occur in regions of discontinuous permafrost, though some may also occur in continuous permafrost regions. These pingo types form by the movement of water under a hydraulic gradient in an intra-permafrost or sub-permafrost aquifer. Thus, these pingo types commonly occur in areas with topographic relief, such as lower hillslopes, alluvial fans, fluvial valleys, and in some cases weathered bedrock as well as rebounding marine terraces (Müller, 1959; Holmes et al., 1968; Yoshikawa and Harada, 1995; French, 2007).

Mackay (1978, 1979, 1998) described the contemporary dynamics of hydrostatic pingos on the Tuktoyaktuk Peninsula, Western Arctic Coast, Canada. These pingos have been shown to form and grow rapidly in lake basins following drainage. Mackay (1998) found that pingos attain their basal diameter early on and subsequent growth is primarily in an upward direction. In one example, a newly formed pingo grew vertically 6 m in its first 20 years of development, but grew slowly over the next 12 years and gained only an additional meter (Mackay, 1998). Of the 1350 pingos on the Tuktoyaktuk Peninsula (Stager, 1956), only about 50 were actively growing in the 1970s (Mackay, 1973). Mackay (1977) also demonstrated the long-term pulsating behavior of some pingos, undergoing alternating periods of growth and subsidence. Further, Mackay (1998) has described pingo collapse in detail, identifying three primary mechanisms: mass wasting, wave erosion, and thermokarst subsidence, and noted that pingos may also subside or deflate due to sub-pingo water loss (Mackay, 1979). In this case, they develop low subsidence bulges on the periphery that are on the order of 0.2 m in height. Thus, pingos should be viewed as a dynamic periglacial landform.

Mackay (1998) estimated the existence of more than 5000 terrestrial pingos on Earth. This estimate included roughly 1450 located along the western Arctic Coast of Canada (Stager, 1956; MacKay, 1979), 1500 in Alaska (Holmes et al., 1968; Carter and Galloway, 1979; Hamilton and Obi, 1982; Walker et al., 1985; Ferrians, 1988), with the remainder scattered in other regions of Canada (Pissart, 1967; Gurney and Worsley, 1997), Russia (Shumskii and Vtyurin, 1966; Vtyurin, 1975), Spitsbergen (Yoshikawa and Harada, 1995), Greenland (Müller, 1959; Worsley and Gurney, 1996), Svalbard (Yoshikawa and Harada, 1995), Scandinavia (Lagerbäck and Rohde, 1985), China (Wang and French, 1995), and Mongolia (Lomborinchen, 2000). However, a recent analysis of topographic map data covering 3.5×10^6 km^2 region of northern Asia has identified more than 6000 pingos (Grosse and Jones, 2011) and an updated Alaska pingo distribution and number map notes more than 3000 (Jorgenson et al., 2008). Thus, in reality there are likely more than 11,000 known pingos in the northern Hemisphere (Grosse and Jones, 2011).

Of the pingos reported in Alaska, Galloway and Carter (1978) mapped 732 within the National Petroleum Reserve-Alaska (NPR-A), located on the western Arctic Coastal Plain of northern Alaska. This mapping effort was based on analysis of stereo-pair aerial photography acquired during the mid-1950s. Pingos with a minimum height of 3 m were identified in the stereo-photography and a point was marked on 1:250:000 scale topographic map sheets from the Harrison Bay, Ikpikpuk, Meade River, Teshekpuk, and Umiat quadrangles. Pingo locations from these map sheets were then compiled to create the map in Galloway and Carter (1978) and used for subsequent discussion and analysis in Carter and Galloway (1979). The majority of other pingo mapping efforts have also utilized stereo-pair photography, topographic map sheets derived from such imagery, and field reconnaissance. However, with advances in terrestrial land surface mapping technologies over the last several decades, the opportunity exists to expand on past studies and provide more detailed information about landforms by analyzing large geospatial datasets within a Geographic Information System (GIS) framework. Of special interest are new high resolution digital elevation datasets derived from airborne Light Detection and Ranging (LIDAR) or Interferometric Synthetic Aperture Radar (IfSAR) systems that allow very detailed morphometric analyses and inventories of periglacial land surface features over large regions (e.g., Abermann et al., 2010). These data also provide the opportunity for

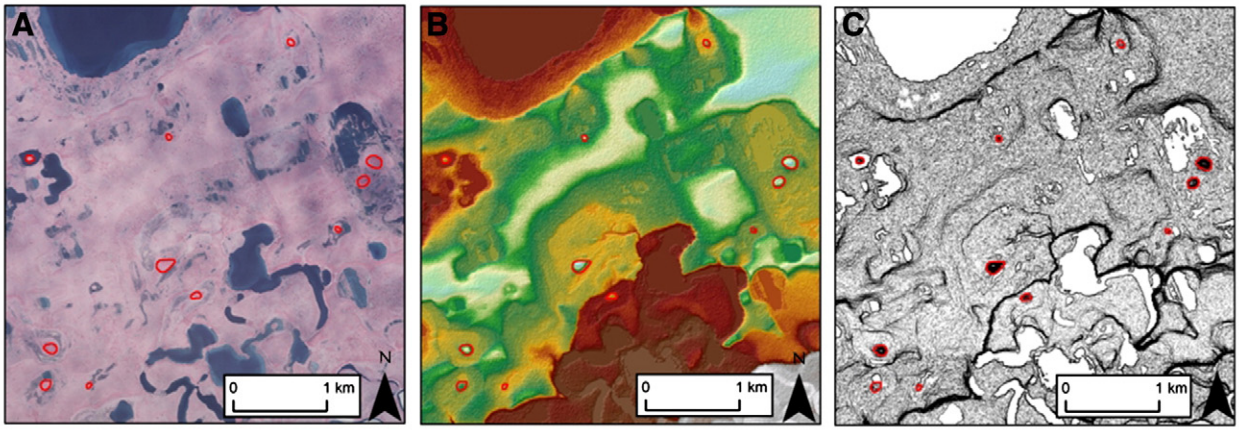

Fig. 2. Comparison of remotely sensed image datasets and derivatives used in this analysis. (A) 2.5 m resolution CIR photography. (B) IfSAR DSM draped over a hillshade derivative. (C) Slope derivative of IfSAR DSM where black indicates greater slope. Pingos are shown as red polygons in each frame.

conducting change detection studies by comparing contemporary and legacy datasets.

Between 2002 and 2006, in a joint effort by the U.S. Geological Survey, the Bureau of Land Management, and the National Science Foundation, a 5 m horizontal resolution and 0.1 m vertical resolution airborne Interferometric Synthetic Aperture Radar (IfSAR) digital surface model (DSM) was acquired over a large portion of the western Arctic Coastal Plain of northern Alaska (Fig. 1). Nolan and Prokein (2003) have previously demonstrated that an IfSAR derived, high-resolution DSM is suitable for identifying a pingo and other periglacial landscape features near Prudhoe Bay, Alaska. Thus, the objective of this study is to conduct a detailed analysis on the distribution of pingos on the western Arctic Coastal Plain in northern Alaska using an IfSAR derived DSM, build a comprehensive dataset of morphometric pingo measurements, and compare this contemporary pingo database with a legacy pingo dataset to identify pingos that may have formed or collapsed over a ~50 year time period.

2. Regional setting and methodology

2.1. IfSAR dataset and pingo mapping

The western Arctic Coastal Plain study region is bounded by the Itkillik River and Colville River Delta to the east, the Beaufort and Chukchi Sea to the North, the extent of the IfSAR derived DSM to the west, and the boundary between the Arctic Coastal Plain and Foothill physiographic provinces to the south (Fig. 1). The raw data were collected with a STAR-3i airborne synthetic aperture radar system, a high-resolution, single pass, across track IfSAR system (Intermap, 2010). The STAR-3i system is capable of acquiring imagery with a horizontal accuracy better than 2 m, a vertical accuracy better than 1 m, and a vertical resolution on the order of 0.1 m (Intermap, 2010). The IfSAR raw data were processed into rectangular tiles covering approximately 200 km^2 each. The final IfSAR DSM product was delivered at a nominal spatial resolution of 5 m. Thus, a total of 315 tiles were needed to create a mosaic that covered our 40,000 km^2 study area. Also available for the entire study region was a 2.5 m resolution, color infrared (CIR), digital orthophoto dataset acquired between 2002 and 2007. The orthophotos were useful in verifying the interpretation of pingos extracted from the IfSAR DSM and for mapping potential pingo remnants and scars.

Mapping of pingos consisted of creating slope and hillshade derivatives of the entire IfSAR dataset (Fig. 2). A 1 km^2 grid was overlain on the study region to systematically identify pingos, which were manually digitized at a scale of 1:5000 from the IfSAR dataset and derivatives as a polygon vector file. Once this dataset was complete, the polygon vector file was converted to a binary raster file (pingo versus non-pingo) and imported into the commercial software package eCognition® to calculate a number of shape metrics. In particular, shape metrics describing length, width, and length-to-width ratio, all measured by a bounding box approximation, were derived. Compactness or circularity, which is defined as the ratio of the area of a polygon to the area of a circle with the same perimeter, was determined by:

$$circularity = \frac{4\pi\, area}{perimeter^2} \quad (1)$$

This index is useful for describing the planimetric shape of a pingo, with values of 1.0 representing a perfect circle, and more irregular shapes having decreasing values. Pingo orientation or direction of the major axis in planimetric shape was also determined for each pingo.

In addition to these shape metrics, a number of other morphometric parameters were determined within the GIS. The elevation of each pingo (in meters above sea level) was determined using a zonal attributes tool that summarized values from the IfSAR DSM raster that fell within a given pingo polygon. Similarly, the mean, maximum, and minimum slope characteristics of each pingo were derived from the slope dataset. Pingo heights were determined by subtracting the mean elevation of a 10 m buffer surrounding a pingo from the maximum elevation value found within a pingo. Finally, the true surface area, planimetric area, and surface ratio (defined as true surface area versus planimetric area) were determined for each pingo with the DEM surface tools extension (Jenness, 2010) for ArcGIS®. In addition to deriving morphometric characteristics of each pingo, we also manually digitized all drained lake basins in which pingos were identified to investigate if pingo metrics were related to basin metrics.

To assess the accuracy of the pingo map and potential errors of commission and omission, we conducted aerial reconnaissance and ground surveys of the study area between 2005 and 2010, and a limited coring campaign in 2007. This effort consisted of flight lines covering approximately 2000 km of the study region and accounting for more than 70% of the IfSAR tiles.

2.2. Legacy pingo and surface geology datasets

The initial pingo distribution map created by Galloway and Carter (1978) consisted of the identification of pingos taller than 3 m from mid-1950s black and white stereo-pair aerial photography, located between the Colville and Usuktuk Rivers. In all, 732 pingos and pingo-like forms were identified within the NPR-A. In addition to these

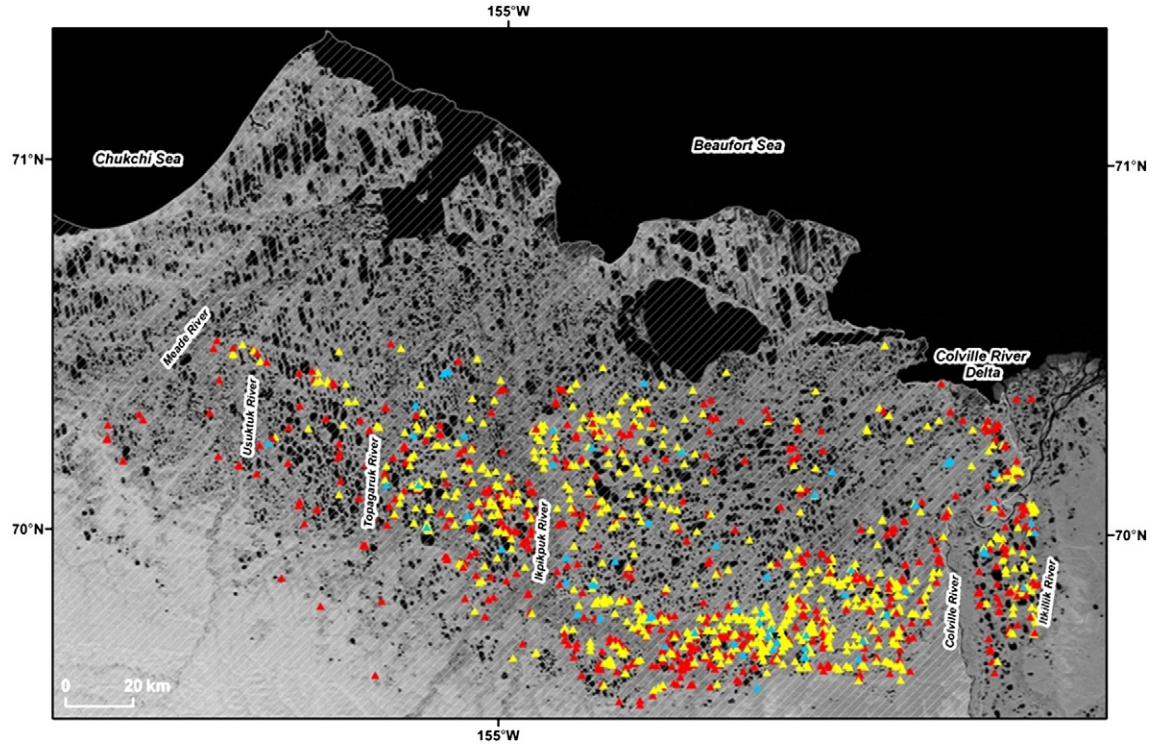

Fig. 3. Map showing the distribution of pingos in the study region. Pingos initially mapped by Galloway and Carter (1978) are shown as a yellow triangle, those additionally mapped in our study as a red triangle, and pingos that potentially collapsed between ca. 1955 and ca. 2005 as a blue triangle. The NPR-A is the region to the west of the Colville River.

previously reported pingos, 80 pingos were identified between the Colville and Itkillik Rivers, yet did not factor into the estimate for the NPR-A since they lay outside the boundary (Galloway, unpublished data).

The original topographic maps that Galloway and Carter (1978) used to mark the location of pingos and pingo-like features were scanned at 1200 dpi and georeferenced to U.S. Geological Survey digital raster graphics. Pingos and pingo-like features were then manually digitized as a point vector file in the GIS. This resulted in a digital legacy dataset with 812 pingos based on mid-1950s remotely sensed imagery. The point file was then compared to the pingo database created from the ca. 2005 IfSAR DSM.

In addition to the pingo legacy dataset, we also georeferenced and digitized the preliminary surficial geology deposits map from Williams et al. (1977). The compiled surface geology map was referenced to the recent CIR photography, and six distinct units were identified within the study region: (1) eolian sand>15 m thick, (2) eolian sand>15 m thick but reworked by streams, (3) marine sand<15 m thick, (4) upland silt, (5) marine silt, and (6) floodplain and fluvial terrace deposits (Table 1). This dataset was used to analyze the distribution and density of pingos with respect to the underlying surface geology. This assessment was limited to pingos located inside the NPR-A since this formed the extent of the Williams et al. (1977) mapping effort.

3. Results and discussion

3.1. Pingo distribution

Our analysis of pingos with the IfSAR DSM and the slope and hillshade derivatives has yielded 1247 pingos taller than 2 m and larger than 30 m^2 in diameter, within the 40,000 km^2 study area on the western Arctic Coastal Plain (Fig. 3). The pingos are interpreted as hydrostatic in origin forming primarily in the confines of drained lake basins (Fig. 4), with 98% distributed within 995 drained basins. The remaining 2% appear to be associated with river meander scars and paleo-river channels. However, these may have formed in a drained basin that could not be distinguished in the remotely sensed imagery. Similarly, Stager (1956) found that 98% of the pingos located on the western Arctic Coast of Canada have formed within drained lake basins, while Mackay (1988) and Marsh et al. (2009) further verified the similarity in the distribution of pingos and drained lake basins on the landscape. Of the 995 drained lake basins with pingos, 86% contain one pingo, 10% contain two pingos, 4% contain more than two pingos, and three basins contained seven pingos. The presence of multiple pingos within a drained lake basin indicates complex lake histories with variable bathymetric and talik geometries within basins resulting in numerous remnant ponds following partial drainage, or possibly heterogeneity in sediments underlying the basin. Interestingly, 97% of the pingos are located in a region for which lakes were suggested to be of non-thermokarst origin (Jorgenson and Shur, 2007).

The location of pingos within drained lake basins indicates that conditions for pingo formation are more favorable near the center of a basin, with the mean distance between the pingo and basin center of 175 m, with a minimum distance of 1 m and a maximum distance of 1.4 km. Likely of more importance is the distance between a pingo and the nearby shallow, remnant pond that commonly results from a lake drainage event (Mackay, 1988). An analysis of pingo location relative to surface water features (derived from zero slope features in the IfSAR DSM) shows that the mean distance to a nearby waterbody is 146 m, with a minimum distance of 1 m and a maximum distance of 1.2 km. Further, more than half of the pingos are located adjacent to remnant ponds or are completely surrounded by water, which is similar to the findings of Stager (1956) for the western Arctic coast of Canada. This comparison highlights the notion that remnant ponds and deeper pools tend to be located near the basin center and, because of this, pingos tend to be centrally located within a basin. This finding is consistent with a number of pingos studied by Mackay (1979) on the Tuktoyaktuk Peninsula.

Table 1
Surficial geologic units in the NPR-A (modified from Williams et al., 1977) in relation to pingo distribution and density.

Surficial deposit	Deposit symbol	Description of materials	Unit distribution and thickness	Topography and drainage	Permafrost	Number of pingos	Planimetric area of unit (km^2)	Percent of pingos in NPRA	Pingos (km^{-2})
Eolian sand>15 m thick	Qes	Fine to medium sand containing abundant quarts with minor dark minerals; chert is locally common. Well sorted. Stratified to massive with large-scale cross bedding in places.	Widespread distribution as a mantle of overlying older marine and other unconsolidated deposits in an area of dunes bordering Meade River extending eastward to Judy Creek. Thickness ranges from 18 to 30 m.	Generally well drained dune ridges as much as 30 m high. Also contains poorly drained to undrained depressions that are not part of an integrated drainage system.	Permafrost underlies entire unit. Volume of wedge and interstitial ice is probably much less than in marine silt and sand units and in upland silt. Thaw settlement largely unknown.	701	12,733	61.4	0.06
Eolian sand>15 m thick; reworked by streams	Qesr	Similar to Qes; however indicates unit that has been reworked by fluvial and thermokarst lake processes	Similar to Qes	Similar to Qes; area of reworked eolian plain with numerous thermokarst lakes	Similar to Qes; pingos are common in drained lake basins	217	1225	19.0	0.18
Marine sand<15 m thick	Qms	Fine to medium sand containing pebbles and granules of chert; also includes silty or clayey sand, sandy silt, and minor beds and lenses of organic material. Massive to poorly stratified.	Forms the relatively flat part of the coastal plain formerly occupied by shallow seas, barrier islands, bars, and spits. Thickness normally 3 to 6 m. Extensively reworked by thermokarst lake activity.	Forms lake dotted coastal plain. Drainage locally good in residual knolls of undisturbed marine sand, but poor in thermokarst lake basins that contain reworked sand, silt and organic deposits	Contains ice wedges and very high volume of ice as small interstitial masses and lenses. Ice content is greater than volume of natural voids down to about 6 m.	52	8273	4.6	0.01
Floodplain and low terrace deposits	Qal	Well sorted, stratified to lenticular deposits of gravel, sand, and silt, generally becoming finer downstream.	Includes floodplain and low terraces (less than 10 m high) bordering streams. Thickness ranges from 1 to 25 m.	Forms terraced plain, part of which is occupied by stream channel and bars, the rest by terraces. Drainage generally poor. Subject to seasonal flooding to 6 or 8 m above low water on many rivers.	Ice content of permafrost in generally granular deposits probably less than in finer materials, even though ice wedges are well developed, especially on terraces. Ice content not known.	115	7527	10.1	0.02
Upland silt	Qs	Silt, silty sand, and fine sand, including some clay and scattered pebbles and granules of chert. Stratification indistinct. Map unit includes windblown silt, thermokarst lake deposits, silt reworked in gullies by running water, and marine (?) silt.	Lies between 45 and 100 m above sea level in an east–west belt at the boundary between the coastal plain and foothills. Deposit a few cm to more than 30 m thick; covers sand and fine gravel of fluvial origin in valleys carved in bedrock.	Forms flat to gently rolling terrain broken by ravines, stream valleys, and thermokarst lakes. Drainage generally poor, except on steep slopes and hill crests	Contains ice wedges and a very high volume of ice as small interstitial masses and lenses. In some areas, ground ice may approach 80% over the volume of subsurface materials, and excess ice may persist to depths great than 30 m below surface.	57	5518	5.0	0.01
Marine silt	Qm	Sandy silt containing scattered pebbles and beds and lenses of sand, clay, pebbly sand, and fine gravel.	Deposit generally limited to within 30 km of present coast. Thickness ranges from 10 to 25 m. Extensively reworked by therkmokarst lake activity	Forms flat, lake-dotted coastal plain lower than 15 m above sea level. Drainage of surface generally poor.	Most of unit has very high content of interstitial ice and small ice lenses; deposit probably has ice in excess of volume of voids down to 6 to 8 m below surface.	0	2449	0.0	0.00

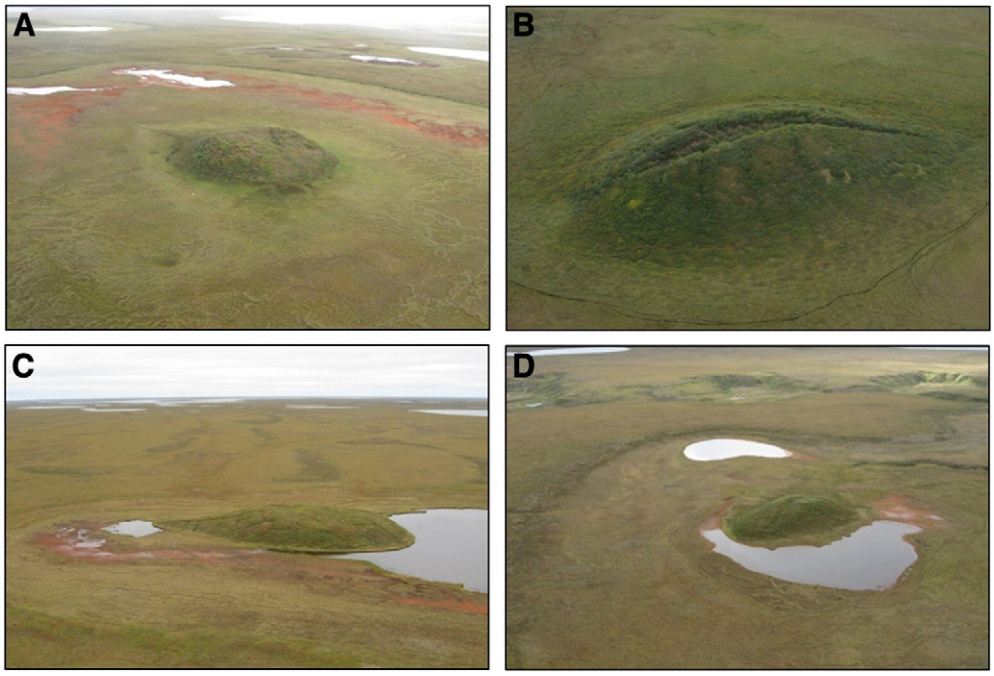

Fig. 4. Oblique photos showing a series of hydrostatic pingos that have formed in drained lake basins: (A) pingo 902, (B) pingo 1105 (Mackay Pingo), (C) pingo 843, and (D) pingo 1143.

Analysis of the 1142 pingos (92% of the total population) located within the NPR-A shows that 61.4% of the pingos occur in eolian sand that is >15 m thick, 19.0% in stream-reworked eolian sands also >15 m thick, 4.6% in marine derived sands <15 m thick, 10.1% in floodplain and low terrace deposits with sandy alluvium, 5.0% in basins formed in upland eolian silt deposits, and none occurring in the northern, marine silt deposits of the outer coastal plain (Table 1). The distribution of pingos in relation to surface geology compares well with the analysis of pingos in northern Asia. Grosse and Jones (2011) found that 68% of the pingos were located in areas underlain by sandy to silty sandy substrates, whereby 12% were associated with alluvial and floodplain deposits. Mackay (1998) also discussed the preferential formation of pingos in areas underlain by thick sandy sediments, which had been subsequently overlain by a layer of finer material deposited during the active lake stage. This distribution of pingos by surface geology differs somewhat from Carter and Galloway (1979) and is likely due to 1) the inclusion of the stream-reworked eolian unit, 2) possibly more accurate delineation of the surface geology units within the GIS, and 3) and inclusion of more pingos on the landscape (435 more than reported in Carter and Galloway, 1979). Our analysis also differs somewhat from the pingo dataset in Jorgenson et al. (2008) in that we did not identify any pingos in the northern, marine silt unit.

Although the greatest number of pingos occur in eolian sand deposits, this constitutes the most extensive surface geology unit in the study region. When analyzing pingo density by surficial geology, the highest density of pingos occur in stream-reworked eolian deposits (nearly 0.18 pingos km^{-2}), with all other types having less than 0.06 pingos km^{-2} (Table 1). The high density of pingos over stream-reworked eolian deposits may be due to selective sorting for somewhat coarser grains and better hydraulic sorting resulting in higher porosity and permeability in the fluvial sand bodies. These results compare well with hydrostatic pingo densities from other regions when based on surface geology units, with densities ranging from 0.01 to 0.28 pingos km^{-2} (Walker et al., 1985). However, Stager (1956) reported higher densities (0.82 pingos km^{-2}) in some areas of the Mackenzie Delta in Canada. Hydraulic pingo densities are also typically less than 1 pingo km^{-2} (Holmes et al., 1968), although densities of >10 pingos km^{-2} have been reported for some regions in Greenland (Worsley and Gurney, 1996).

3.2. Pingo morphometry

The mean height of all 1247 pingos was 4.6 m and 95.5% of the pingos are less than 10 m high (Fig. 5). Pingo heights ranged from a low of 2 m (minimum mapping unit height) to a high of 21 m (Fig. 6). Carter and Galloway (1979) also reported that the tallest pingo in their mapping effort to be 21 m, thus providing evidence of general agreement between the two datasets. Further, Grosse and Jones (2011) recently reported a

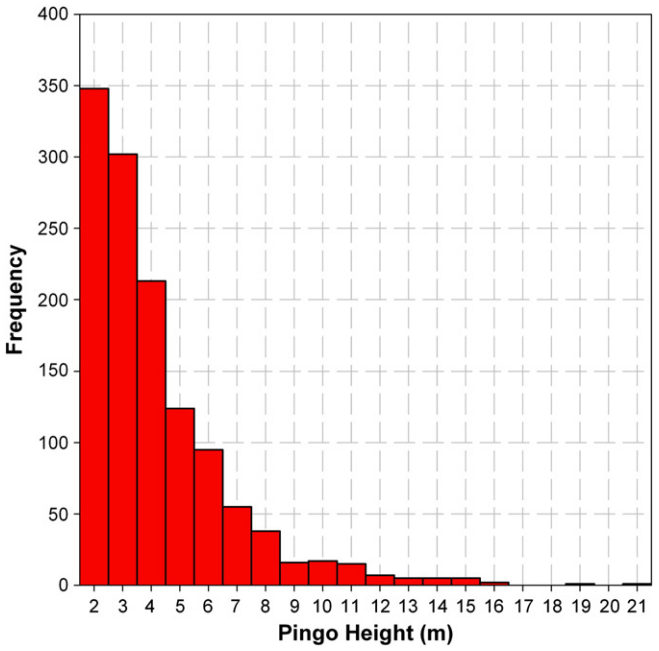

Fig. 5. Histogram of pingo heights for the 1247 pingos taller than 2 m.

mean pingo height of 4.8 m for more than 3000 pingos in northern Asia. Thus, while it is known that the tallest pingos on earth are on the order of 40 to 50 m, they are likely the exception and pingos on the order of 5 m in height are likely more common.

Pingo diameter ranged from 32 to 295 m with an average of 94 m. The mean length-to-width ratio is 1.3, indicating that pingos in our study region tend to be circular to slightly elliptical in shape. However, 10% of the pingos had a major-axis two times longer than the minor-axis, producing a more elongate shape. Circularity or compactness shows that the mean value for all pingos was 0.88 (1.0 being a perfect circle), with values ranging from a low of 0.30 to a high of 0.98 (Fig. 7A).

The planimetric area of pingos ranged from 775 to 68,500 m^2 with a mean of 8000 m^2. Surface area measurements show a range of 780 to 69,000 m^2 and a mean of 8100 m^2. Taking the ratio of surface area to planimetric area, otherwise known as surface ratio or rugosity, provides a measure of the ruggedness of a pingo, with values closer to 1.00 being nearly identical measures and indicating smooth, planar morphology. For our dataset, the mean difference in true surface and planimetric area is 1%; however, some pingos had 15% more surface area when compared to planimetric area and a trend towards increasing surface ratio or ruggedness with pingo height is observed (Fig. 7B). Point measurements of slope show that values ranged from 0° near base and summit, to a maximum slope of 57° along the pingo flanks. Mean pingo slopes ranged from 1.5° to 20° for all 1247 pingos.

Many different pingo forms are evident in our study region (Fig. 8). Using values given in Mackay (1988), pingos were divided into three size classes with small pingos defined as those <100 m in diameter, medium pingos as those with 100–200 m diameter, and large pingos as those >200 m in diameter. This analysis demonstrates that 760 (61%) of the pingos in the study area are small, 445 (36%) are of medium size, and 42 (3%) are large. Mackay (1988) also distinguished between steeply (> 30°), moderately (15° to 30°), and gently (<15°) sloping pingos. Applying this scheme to the pingos in the study area shows that 759 (61%) are gently sloping, 462 (37%) are moderately sloping, and only 26 (2%) are steeply sloping. We could not identify in the literature where pingos were divided in various height classes, other than hypothetical values given in Stager (1956). For this reason, we devised our own scheme and further analyzed our dataset based on short (2 to 5 m), medium (5 to 10 m), and tall (>10 m) pingos. Short pingos accounted for 862 (69%), medium pingos for 328 (26%), and tall pingos for 57 (5%). Thus, the majority of the pingos on the western Arctic Coastal Plain may be considered to be small to medium in size, gently to moderately sloping, and of a relatively short stature (Table 2).

We also delineated the drained basins in which 98% of the pingos had formed. The 1219 pingos taller than 2 m were distributed across 995 basins. As mentioned earlier, single pingo basins are the norm, although a few basins contained as many as seven pingos. In order to examine whether pingo and basin size and orientation were related, we compared the two metrics. In general, as the maximum basin diameter increases so does the pingo diameter (Fig. 9A). Thus, the larger pingos tend to be found in the larger drained basins. Mackay (1979) found that in order for a pingo to form in a basin, the basin diameter had to be at least four times larger than the pingo diameter to supply sufficient pore water. The comparison of this metric in our study area shows that all pingo versus basin diameters meet this criterion. When comparing pingo orientation with basin orientation it is obvious that there is no relation (Fig. 9B).

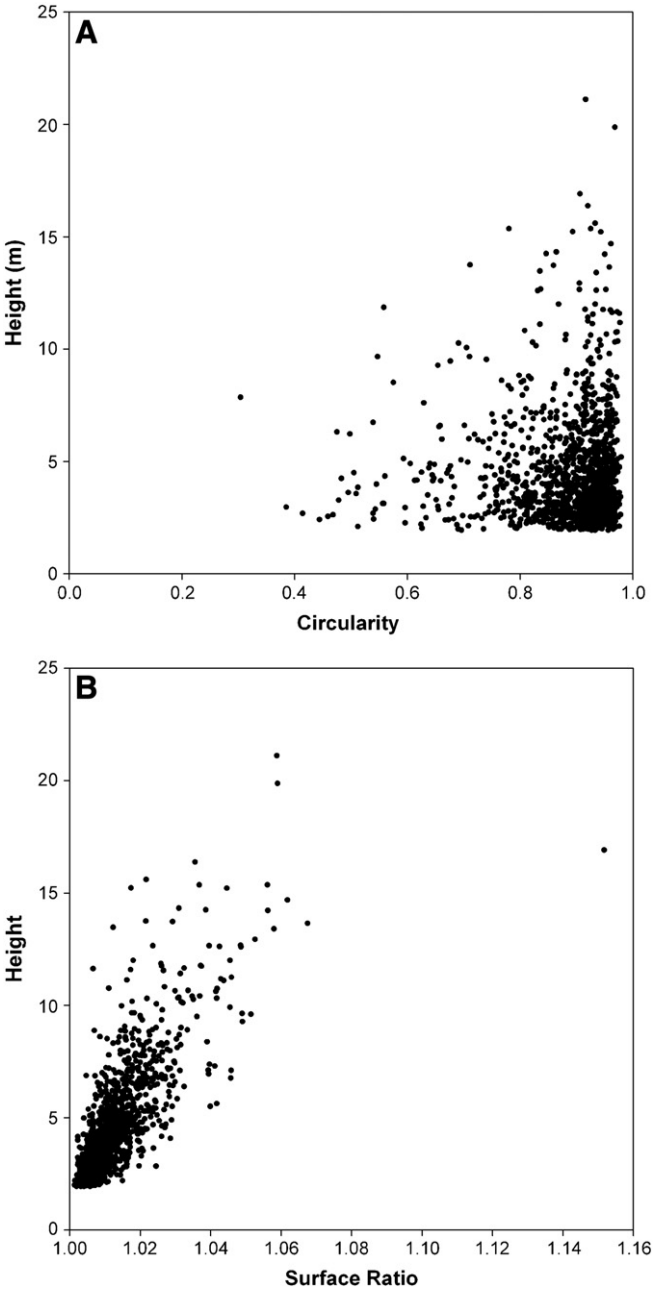

Fig. 7. Scatterplot showing (A) circularity versus height and (B) surface ratio versus height. Most pingos are circular to slightly elongate (mean of 0.88) and the difference between surface and planimetric area increases with height.

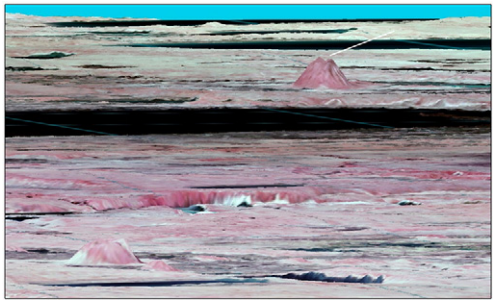

Fig. 6. Three-dimensional perspective of the CIR photography draped over the IfSAR DSM with a 2× vertical exaggeration. The pingo in the foreground is 5 m tall and the pingo in the background is 21 m tall, the tallest in the region. This pingo (pingo 1105), informally named Mackay Pingo, is also shown in Figs. 4B and 8B. Note that the horizontal and vertical resolution of the DSM is able to resolve the dilation crack (white line) that runs lengthwise along this pingo.

3.3. Pingo database accuracy

We have been able to conduct an accuracy assessment of the IfSAR derived pingo database over the last several years. We have overflown a

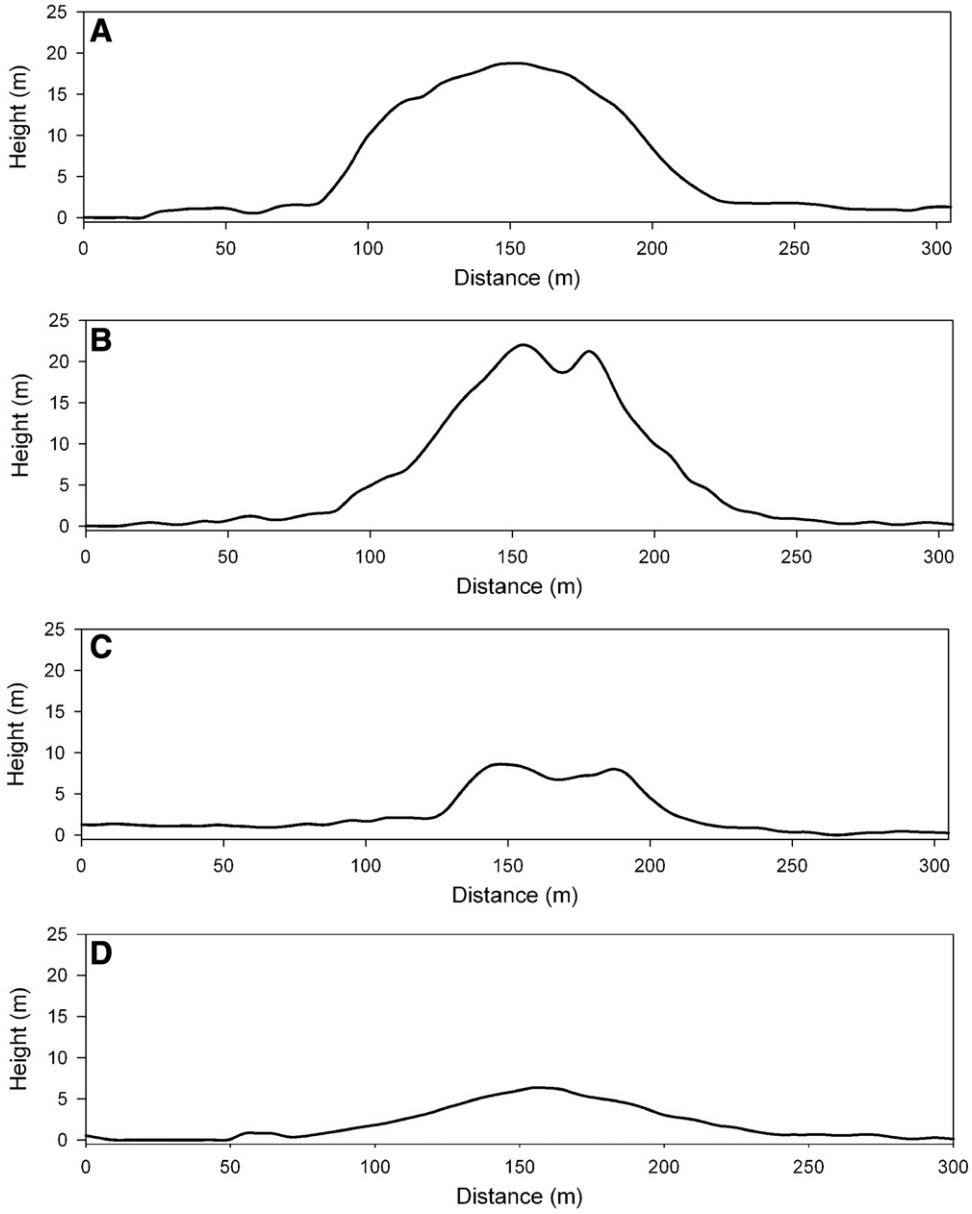

Fig. 8. Topographic cross-section profiles of select pingos within the study region. (A) Pingo 1078, a tall, rounded pingo form. (B) Pingo 1105 (Mackay Pingo), a tall, steeply sloped pingo with a well-defined dilation crack. (C) Pingo 1226, an average height pingo with a ruptured summit. (D) Pingo 586, an average height pingo with a gentle slope and possible subsidence bulge.

total of 300 pingos (roughly 24% of the pingos in the study region) and found that our IfSAR analysis failed to identify only one pingo taller than 2 m along the flight paths while misclassifying three; these turned out to be erosional landscape remnants instead of pingos. If similar errors of omission and commission apply to the remainder of the pingo population, then the accuracy of our pingo dataset likely exceeds 98%. During a short field excursion in the summer of 2007, we were also able to acquire near-surface sediment cores from five pingo summits. In all cores, we encountered what appeared to be injected ice bodies within the upper 2 m of each feature, leading us to believe that we have indeed mapped pingos as opposed to erosional remnants.

There is also a possibility that some of the pingo forms that we identified may be palsas, lithalsas, broad-based mounds, or seasonal frost mounds. After our initial classification of pingo forms, we removed 149 because the height of the feature was below 2 m or the basal diameter was less than 30 m. Removal of these features limited the inclusion of smaller frost mound types in our pingo analysis. However, without ground truth data distinguishing palsa and lithalsas from pingos, we cannot definitively rule out this possibility. Palsas have been reported in some locations along the Dalton Highway to the east of our study area (Nelson et al., 1985; Outcalt et al., 1986) and in the Arctic Refuge near the Canadian border (Tsuyuzaki et al., 2008). In both areas, palsas tend to be on the order of 1 m tall or shorter. Walker et al. (1985) described broad based mound features near Prudhoe Bay, Alaska. Comparing measurements of slope and height versus mean diameter shows that some of our features potentially fall in the range of sizes (larger) and slopes (lower) given for these anomalous features (Fig. 10). However, Walker et al. (1985) noted that none of the broad based mounds in their study area had formed in drained lake basins, whereas these larger and more gently sloping features in our study region were

Table 2
Metrics (basal diameter, pingo height, flank slope, pingo circularity, proximity to pond, and location within basin) used for describing and categorizing pingo characteristics.

Metric	Pingo characteristics	Number of pingos	% of pingos
Basal diameter	Small (<100 m)	760	61
	Medium (100 to 200 m)	445	36
	Large (>200 m)	42	3
Pingo height	Short (2 to 5 m)	862	69
	Medium (5 to 10 m)	328	26
	Tall (>10 m)	57	5
Flank slope	Gently sloping (<15°)	759	61
	Moderately sloping (15° to 30°)	462	37
	Steeply sloping (<30°)	26	2
Pingo circularity	Circular (>0.9)	704	56
	Intermediate (0.6 to 0.9)	514	41
	Elongate (<0.6)	29	2
Proximity to pond	Proximal (<100 m)	669	54
	Intermediate (100 to 500 m)	539	43
	Distal (>500 m)	39	3
Location within basin	Within lake basin	1219	98
	Outside lake basin	28	2

all located within drained lake basins, further indicating that these are likely pingos, and that many such pingo forms exist. Given the fact that palsas are seldom described on the western Arctic Coastal Plain, that broad-based mounds have not been found in drained lake basins before, and that we removed all pingo-like features shorter that 2 m, we believe we have only mapped pingos in our database.

3.4. Comparison with legacy pingo dataset

Pingo mapping efforts by the U.S. Geological Survey in the late-1970s using aerial photography acquired in the mid-1950s identified 812 pingos taller than 3 m in the study region (Galloway and Carter, 1978; Carter and Galloway, 1979; Galloway, unpublished data). Comparison of the database created from this legacy dataset with information derived from the IfSAR DSM indicates that 45 pingos may have completely collapsed or deflated between the mid-1950s and mid-2000s as these features were not distinguishable (Figs. 3 and 11). An additional 21 pingos may have substantially subsided or deflated as their heights measured from the ca. 2005 IfSAR dataset were more than 1.5 m below the minimum cutoff height used in the initial mapping effort.

An effort was made to identify the mechanisms that may have led to pingo collapse. Although difficult to distinguish in the remotely sensed imagery, it appears that many have simply deflated or subsided, possibly due to loss of sup-pingo water lens pressure as described by Mackay (1979). Alternatively, the role of strong directional winds as well as excavations of the pingo surface by ground squirrels and foxes may act as erosional mechanisms that ultimately lead to the full or partial collapse of a pingo (Mackay and Burn, 2011). However, the possibility exists that many of these features were erroneously identified in the legacy dataset, or the points marked on the topographic map sheets were mislocated. Further, it is difficult to determine the potential error in estimating pingo heights between the initial mapping effort and our more recent effort, even though both approaches found the tallest pingo in the region to be 21 m, which suggests some agreement between the methodologies.

Comparing the total number of pingos mapped in the earlier effort with those mapped here shows that we have identified an additional 435 pingos. This is in part due to the fact that we used 2 m as our minimum mapping unit height, whereas Galloway and Carter (1978) used 3 m. However, of the additional pingos mapped in the study region only 193, or less than half, fall within the 2 to 3 m height class. Thus, it is likely that the additional pingos we identified were either overlooked in the initial study, or have formed subsequent to the mid-1950s.

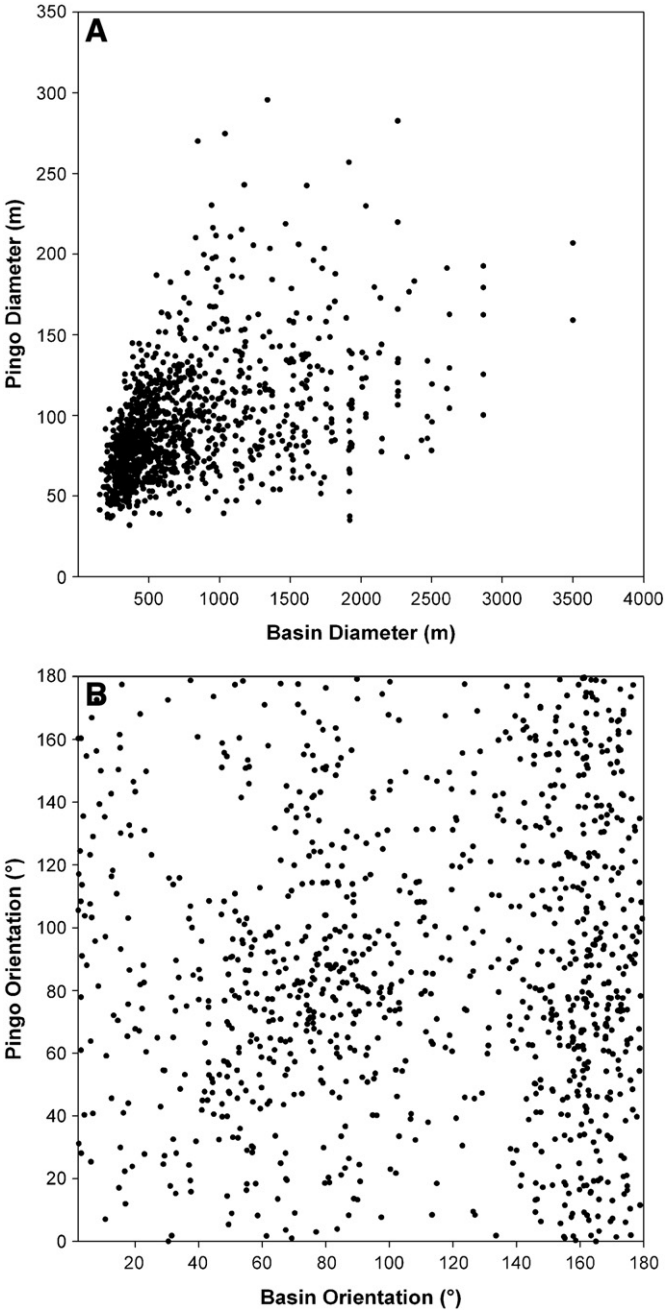

Fig. 9. Scatterplot showing comparison between (A) mean basin and pingo diameters and (B) basin and pingo orientations.

As noted above and elsewhere, pingo formation in the region is intimately tied to lake drainage. Hinkel et al. (2007) found that 50 lakes drained within this study region between 1975 and the early 2000s. Of these 50 lakes, we only detected two that have spawned the growth of a pingo higher than 2 m, and both sites are located within the thick eolian sand deposits. It is possible that shorter pingo-like features have formed following drainage and that they are still actively growing upward. However, Mackay (1998) did show that pingos tended to grow rapidly following lake drainage, attaining near maximum heights within a 20 to 30 year time period. Extending this lake drainage history back to the mid-1950s with lake information available on the topographic map sheets shows that we have only been able to positively identify one additional pingo that formed between ca. 1955 and ca. 2005. Thus, the

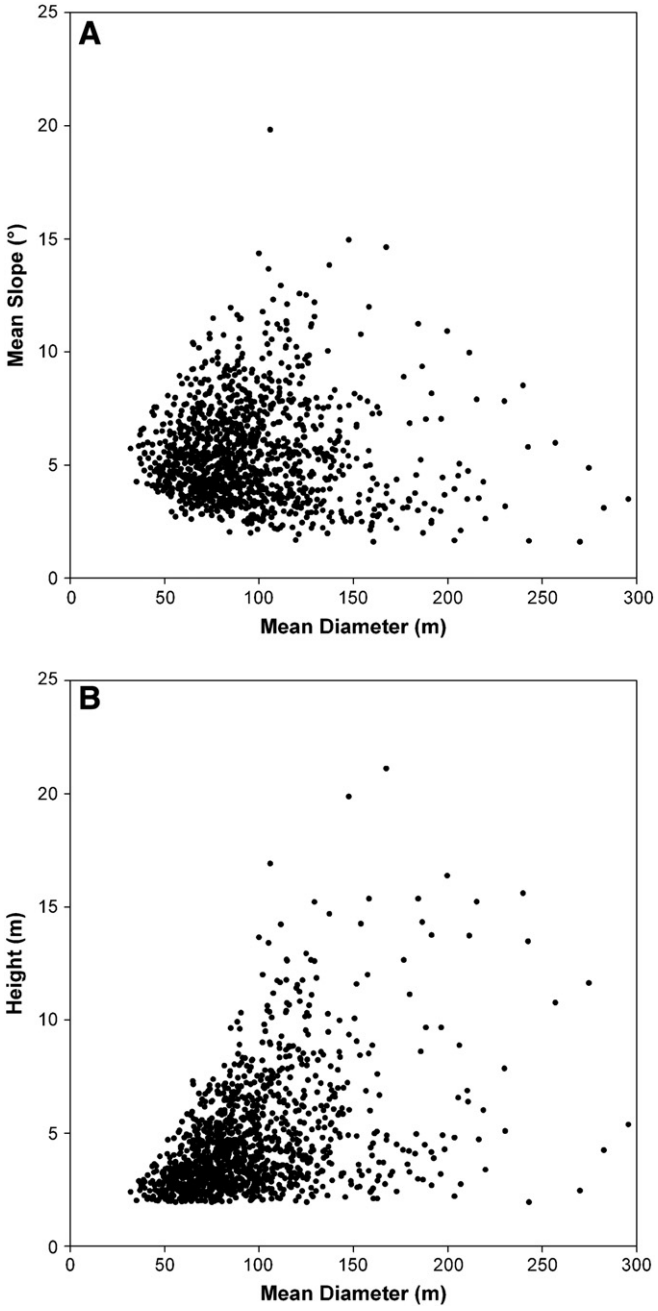

Fig. 10. Scatterplot of (A) mean diameter versus mean slope and (B) mean diameter versus height.

fact that the majority of pingos additionally mapped in our effort were simply overlooked in the initial mapping effort indicates that caution should be taken when comparing contemporary datasets with legacy datasets derived using different methodologies.

Comparing the rate of pingo formation in our region with other regions shows that pingos may form more slowly here. Mackay (1973) found that five new pingos formed between 1935 and the early 1970s in the Tuktoyaktuk region. Extrapolating this to a 100 year time period he suggested the formation of approximately 15 pingos per 100 yrs. Using the same reasoning, a pingo formation rate of six pingos per 100 yrs for the western Arctic Coastal Plain seems more likely although pingo growth is intimately related to lake drainage in this region. Given that some drained lake basins contain up to seven separate pingos it is likely that this rate fluctuates greatly through time. However, it should also be noted the period of observation of Mackay's studies occurred during a cooler climate interval than our observation period.

3.5. Collapsed pingos and pingo scars

Of the 1247 pingos mapped in our study area, 62 (5%) had well-developed, cratered centers, which often contained thermokarst ponds (Fig. 12). Topographic, cross-section profiles show well-developed ramparts along the periphery and a collapsed central basin (Fig. 13). In some cases the ramparts remain elevated 4 to 5 m above the surrounding terrain. While it is common for thermokarst ponds to form in the center of collapsed pingos, they likely account for a relatively minor proportion of the lakes and ponds on the landscape in this region (Cabot, 1947). Bathymetric surveys conducted on three collapsed pingo ponds showed a bowl shaped depression with a mean water depth around 2 m. Interestingly, the bottom of each of the ponds was roughly the same elevation as the surface of the surrounding drained lake basin.

Additionally, we mapped 91 pingo scars visible in the CIR orthophotography, with ramparts below the 2 m height cutoff used in our analysis. It is not clear whether these pingo forms were ever taller than 2 m or when the collapse occurred. However, by adding these pingo scars to the total pingo population we can determine the percentage of the population that is severely degraded. Approximately 7% of our population can be considered severely degraded, comparing well with a similar analysis of pingos from the western Arctic Coast of Canada, where roughly 8% of the pingo population had well-developed craters and were considered to have collapsed (Stager, 1956). Thus, if the proportion of collapsed pingos in a region provide some indication of the age of the features across the landscape, then initial pingo development between these two areas may have commenced synchronously, and likely coincide with the initial formation and drainage of lakes at the beginning of the Holocene.

3.6. Pingo database applications

Information on the location and morphology of pingos on the landscape also has practical applications. Because the western Arctic Coastal Plain is so large and remote, with limited on-the-ground resources such as extensive field surveys, previously there was a general lack of knowledge on modern pingo distribution and morphometry. The pingo database derived from the IfSAR DSM offers assistance in obtaining a more complete and accurate catalog of pingos in the area, but also offers the ability to easily share the data and update it on a regular schedule in a relatively inexpensive and efficient manner with a potentially large audience. Such information can assist in compiling a more complete understanding of the complexity and dynamics of the western Arctic Coastal Plain landscape. The potential use of such a database includes regional planning and assessment efforts, project planning and assessment, identification of archeological sites, and long-term monitoring projects. Practical use at the project level may include conducting spatial analyses using the latest available DSM and the pingo database to assess high points on the landscape as well as view sheds. Such an effort would be useful in planning the most optimum location for short-term deployment of a long-distance, radio-telemetry network of repeater stations. Pingos also provide important habitat (Koranda, 1970), are culturally significant (Lobdell, 1986), and may indicate the location of fault systems and potential infrastructure damage (Wu et al., 2005) and/or access to gas hydrates (Papp et al., 2005; Skirvin et al., 2008).

The up-to-date and comprehensive pingo map for the western Arctic Coastal Plain will also help industry to identify potential hazards (Wu et al., 2005) when planning or designing large development projects in northern Alaska. A typical development

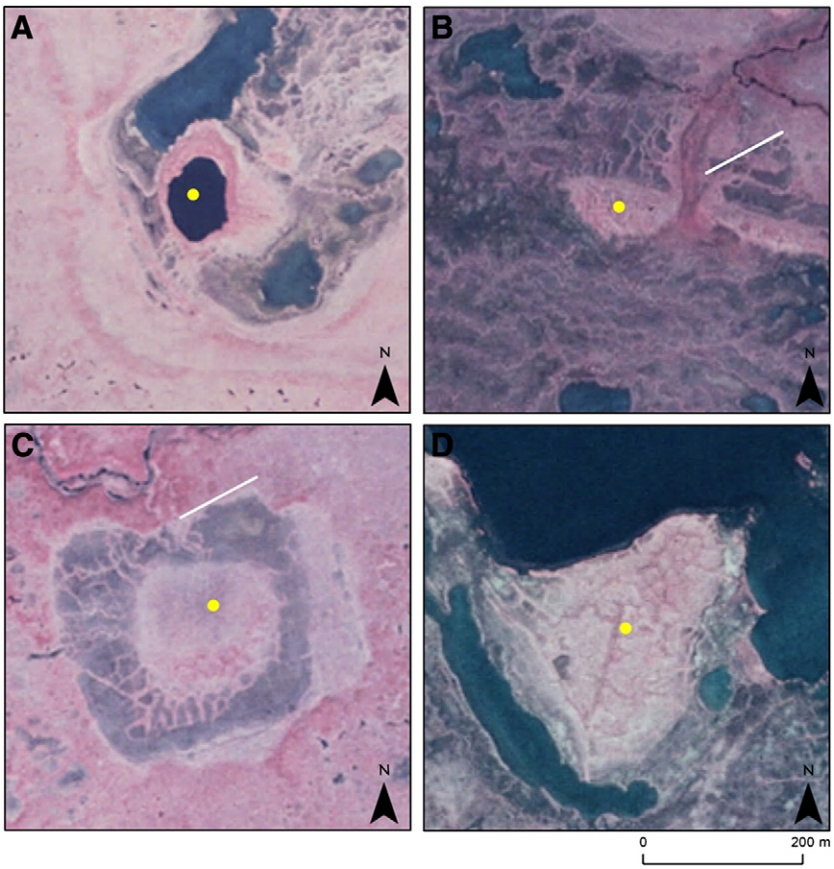

Fig. 11. Examples of pingos that have potentially collapsed between ca. 1955 and ca. 2005. (A) Pingo with a well developed crater and remnant pond. (B) Deflated pingo showing possible signs of spring flow (white line). (C) Another pingo showing possible signs of spring flow (white line) and deflation. (D) Pingo that has been partially eroded by a thermokarst lake.

project in the area may exist to the year 2100, and requires a great deal of planning by a company and analysis by government agencies. One important facet of the planning and analysis for potential projects in this century is the ability to incorporate climatic change at various scales and associated landscape-scale feedbacks. Regular updates of the pingo database with new elevation data will result in

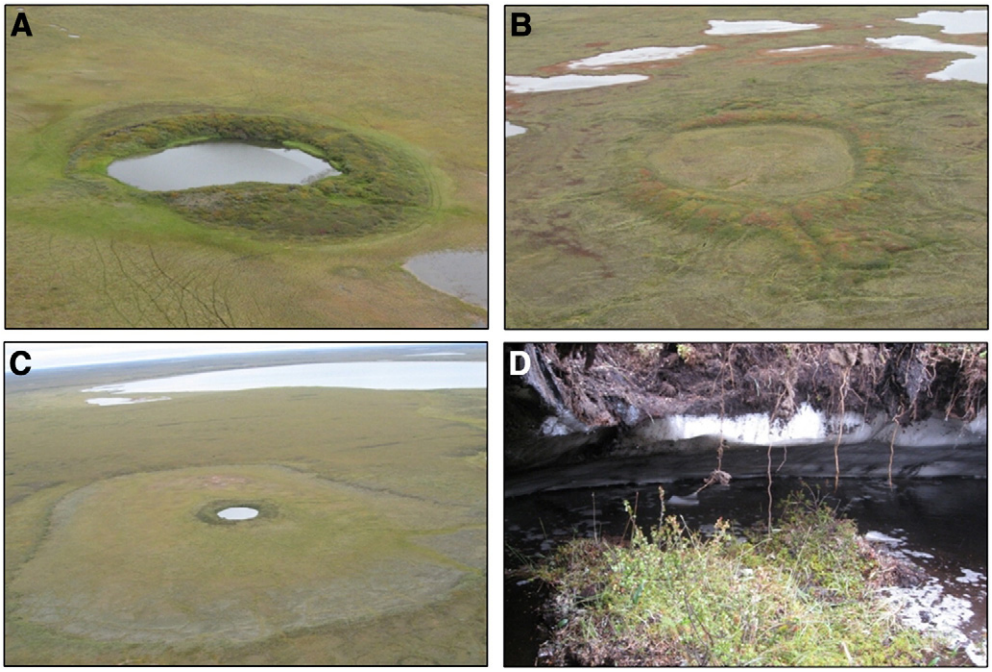

Fig. 12. Field photos of collapsed pingos. (A–C) Oblique photos of pingo scars and remnant pingos occurring in the study region. (D) Ground photo of a collapsing pingo showing the sharp contact between the ice core and overburden.

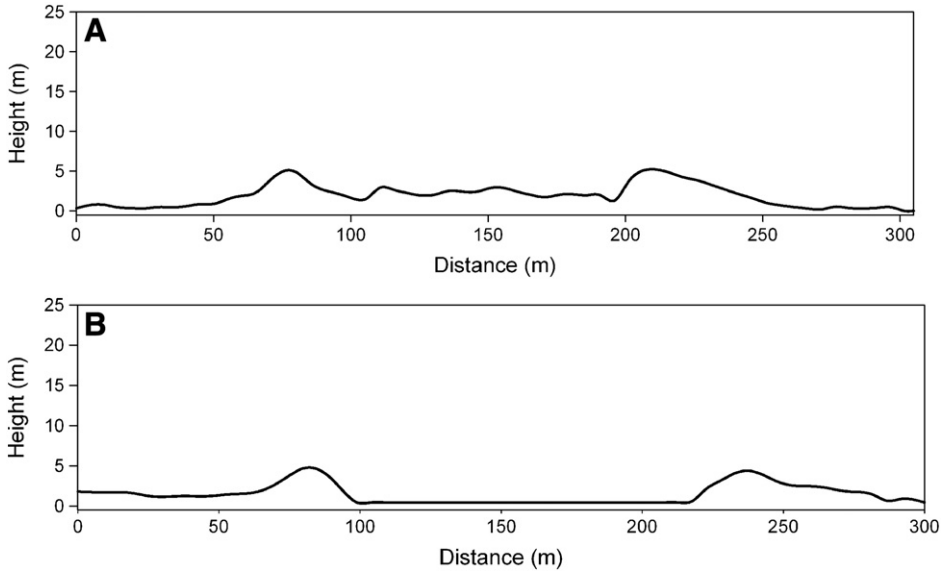

Fig. 13. Examples of cross-sectional profiles of collapsed pingo forms. (A) Pingo having a cratered summit with two small ponds located at the 100 and 195 m distances. (B) Pingo having a cratered summit that is filled with a thermokarst pond.

identification of pingo dynamics, and may offer the ability to use pingos as a landscape-health indicator for a region being altered by climate change. Given the distribution of pingos in the study area, the loss of pingos may present a moderately serious land surface change, which may result in uncertain habitat and wildlife responses.

Pingo-like features (PLFs) also occur in extraterrestrial, periglacial environments such as on Mars (Cabrol et al., 2000; Burr et al., 2005, 2009; Soare et al., 2005). Proof of the existence of Martian pingo analogs may indicate presence of massive ground ice and subsurface water flow on Mars in the past. Dundas and McEwen (2010) have recently questioned the interpretation of a vast number of PLFs on Mars; in many cases they view these features as remnants of differential erosion. Thus, a detailed analysis such as we present on the morphometry of pingos in a periglacial landscape on Earth may prove useful for better identifying pingos on Mars. Burr et al. (2005) provided measurements of circularity versus area and circularity versus perimeter for a number of PLFs in the Athabasca Valles of Mars. Although comparison of these metrics is somewhat difficult because the variables used are not independent (both area and perimeter are used to calculate the circularity value), they show a continuum in form of the PLF they identified (i.e. no discrete grouping). Plotting the same metrics for the pingos in our study region shows a similar trend, with decreasing circularity associated with an increase in planimetric area and perimeter. However, the Pearson product moment of correlation for circularity versus area for our dataset was −0.36 and for circularity versus perimeter it was −0.54 (Fig. 14); whereas, Burr et al. (2005) reports values of −0.66 and −0.81, respectively, for the PLFs on Mars. The lower correlation in our dataset relative to the Martian dataset indicates that some larger pingos may also maintain a more circular form. Thus, information derived from our pingo database may prove useful for interpretation of PLFs in other environments such as on Mars.

4. Conclusion

A recently acquired Interferometric Synthetic Aperture Radar (IfSAR) derived digital surface model (DSM) reveals that there are 54% more pingos on the western Arctic Coastal Plain than previously documented in a legacy pingo dataset for the region, further increasing the number of known pingos in the Northern Hemisphere. Of the 1247 pingos mapped in this study, 98% have formed within drained lake basins indicating that the origin of these two permafrost landforms are closely linked and the vast majority of pingos in the region are of hydrostatic origin. Of these pingos in drained lake basins, 80% have formed where thick eolian sand deposits underlay the surface. The majority of the pingos on the western Arctic Coastal Plain appear to be small to medium in size, gently to moderately sloping, and of a relatively low height. Whereas the tallest pingos on Earth are on the order of 40 to 50 m high, they are likely the exception and pingos on the order of 4 to 5 m in height are likely more common. Comparison of our IfSAR derived pingo database with a legacy dataset based on analysis of mid-1950s vertical, stereo-pair aerial photography indicates that 66 of the pingos initially mapped on the western Arctic Coastal Plain may have collapsed or deflated between the mid-1950s and mid-2000s. Development of similar periglacial landform databases with modern remotely sensed image technologies will help in the identification of similar forms on Mars and provide a useful tool for land and resource managers as they manage the landscape for the impacts of climate change and human pressure.

Acknowledgments

This work was supported by the U.S. Geological Survey–Alaska Science Center, Geographic Analysis and Monitoring Program, and Land Remote Sensing Program. Partial support was provided by the U.S. Fish and Wildlife Service, the Bureau of Land Management, the National Science Foundation under grants ARC-0713813 and BCS-0548846 to KMH, ARC-0640371 to RAB, and OPP-0732735 to GG as well as NASA grant NNX08AJ37G to GG. Any opinions, findings, conclusions, or recommendations expressed in this material are those of the authors and do not necessarily represent the views of the National Science Foundation or NASA. Any use of trade, product, or firm names is for descriptive purposes only and does not imply endorsement by the U.S. Government. We would particularly like to thank Jim Webster of Webster's Flying Service for all of the help and support in the field over the last several years. We also thank Kenji Yoshikawa for critical discussions on pingo mapping techniques. The manuscript further benefited from the reviews of Thomas D. Hamilton, Christopher Waythomas, Jennifer Jenkins, and two anonymous reviewers.

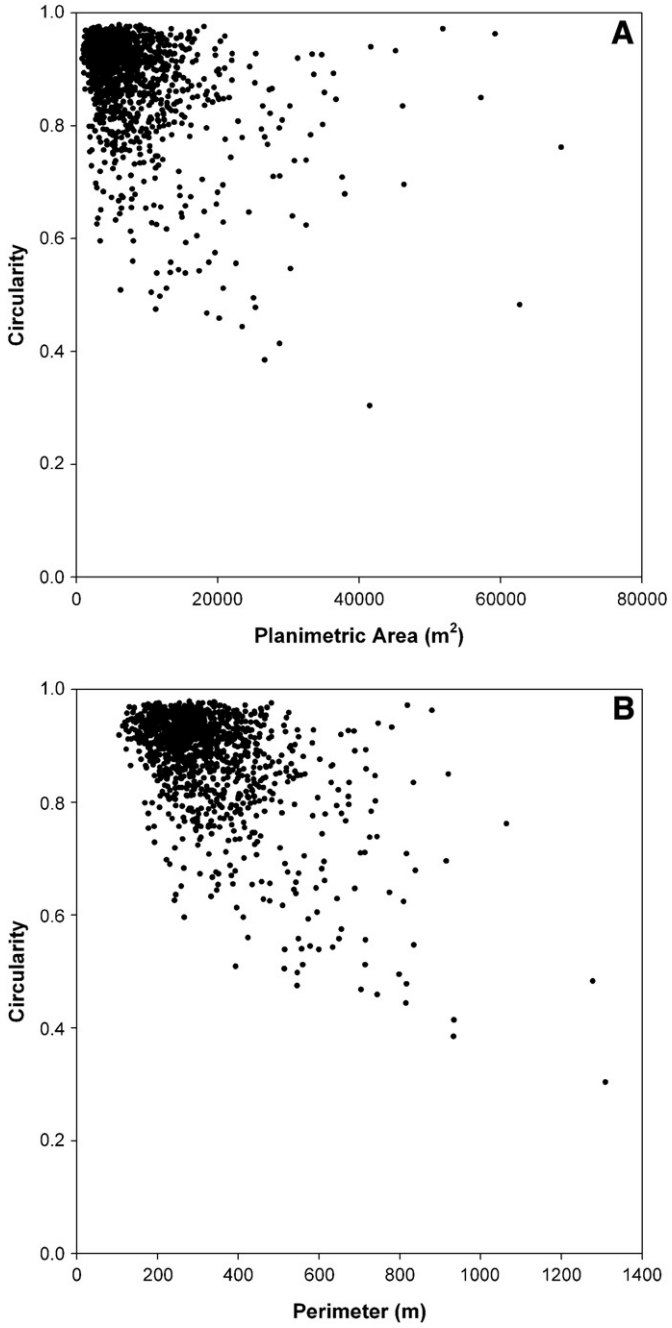

Fig. 14. Scatterplot showing relation between (A) planimetric area and circularity and (B) perimeter and circularity of pingos mapped with the IfSAR dataset for the western Arctic Coastal Plain.

References

Abermann, J., Fischer, A., Lambrecht, A., Geist, T., 2010. On the potential of very high-resolution repeat DEMs in glacial and periglacial environments. The Cryosphere 4, 53–65.

Burr, D.M., Soare, R.J., Wan Bun Tseung, J.M., Emery, J.P., 2005. Young (late Amazonian), near surface, ground ice features near the equator, Athabasca Valles, Mars. Icarus 178, 56–73.

Burr, D.M., Tanaka, K.L., Yoshikawa, K., 2009. Pingos on Earth and Mars. Planetary and Space Science 57, 541–555.

Cabot, E.C., 1947. The northern Alaska coastal plain interpreted from aerial photographs. Geographical Review 37, 639–648.

Cabrol, N.A., Grin, E.A., Pollard, W.H., 2000. Possible frost mounds in an ancient Martian lake bed. Icarus 145, 91–107.

Carter, L.D., Galloway, J.P., 1979. Arctic Coastal Plain pingos in National Petroleum Reserve in Alaska. In: Johnson, K.M., Williams, J.K. (Eds.), The United States Geological Survey in Alaska—Accomplishments during 1978: U.S. Geological Survey Circular, 804-B, pp. B33–B35.

Dundas, C.M., McEwen, A.S., 2010. An assessment of evidence for pingos on Mars using HiRISE. Icarus 205, 244–258.

Ferrians Jr., O.J., 1988. Pingos in Alaska: A review. Fifth International Conference on Permafrost, Norway, pp. 734–739.

French, H.M., 2007. The Periglacial Environment, 3rd ed. John Wiley and Sons Ltd, Chichester, p. 448.

Galloway, J.P., Carter, L.D., 1978. Preliminary map of pingos in the National Petroleum Reserve in Alaska. U.S. Geological Survey, Open-File Report, pp. 78–795.

Grosse, G., Jones, B.M., 2011. The spatial distribution of pingos in northern Asia. The Cryosphere 5, 13–33.

Gurney, S.D., 2001. Aspects of the genesis, geomorphology and terminology of palsas: perennial cryogenic mounds. Progress Physics Geography 25, 249–260.

Gurney, S.D., Worsley, P., 1997. Genetically complex and morphologically diverse pingos in the Fish Lake area south west Banks Island, N.W.T., Canada. Geografiska Annaler 79A, 41–56.

Hamilton, T.D., Obi, C.M., 1982. Pingos in the Brooks Range, Northern Alaska, U.S.A. Arctic Alpine Res 14, 13–20.

Hinkel, K.M., Jones, B.M., Eisner, W.R., Cuomo, C.J., Beck, R.A., Frohn, R., 2007. Methods to assess natural and anthropogenic thaw lake drainage on the western Arctic Coastal Plain of northern Alaska. Journal of Geophysical Research 112, F02S16. doi:10.1029/2006JF000584.

Holmes, G.W., Hopkins, D.M., Foster, H., 1968. Pingos in central Alaska. U.S. Geological Survey Bulletin, 1241-H, pp. H1–H40. Washington, D.C.

Intermap, 2010. Product Handbook and Quick Start Guide, Standard Edition. Intermap, p. v 4.4.

Jenness, J., 2010. DEM Surface Tools for ArcGIS (surface_area.exe). Jenness Enterprises, p. v. 2.1.254. Available at: http://www.jennessent.com/arcgis/surface_area.htm.

Jorgenson, M.T., Shur, Y., 2007. Evolution of lakes and basins in northern Alaska and discussion of the thaw lake cycle. Journal of Geophysical Research 112, F02S17. doi:10.1029/2006JF000531.

Jorgenson, M.T., Yoshikawa, K., Kanevskiy, M., Shur, Y., Romanovsky, V., Marchenko, S., Grosse, G., Brown, J., Jones, B.M., 2008. Permafrost characteristics of Alaska. Proceedings of the Ninth International Conference on Permafrost, Fairbanks, Alaska, 29 June–3 July.

Koranda, J.J., 1970. Pingos. Pacific Discovery 23, 18–24.

Lagerbäck, R., Rohde, L., 1985. Pingos in northernmost Sweden. Geografiska Annaler A 67, 239–245.

Lobdell, J.E., 1986. The Kuparuk Pingo Site: a northern Archaic hunting camp of the Arctic Coastal Plain, north Alaska. Arctic 39, 47–51.

Lomborinchen, R., 2000. Frost heaving and related landforms, Mongolia, Permafrost Periglac. Proceedings 11, 85–90.

Mackay, J.R., 1973. The growth of pingos: Western Arctic Coast, Canada. Canadian Journal of Earth Sciences 10, 979–1004.

Mackay, J.R., 1977. Pulsating pingos, Tuktoyaktuk Peninsula, N.W.T. Canadian Journal of Earth Sciences 14, 209–222.

Mackay, J.R., 1978. Contemporary pingos; a discussion. Biuletyn Peryglacjalny 27, 133–154.

Mackay, J.R., 1979. Pingos of the Tuktoyaktuk Peninsula area, Northwest Territories. Geographie Physique et Quaternaire 33, 3–61.

Mackay, J.R., 1988. Pingo collapse and paleoclimatic reconstruction. Canadian Journal of Earth Science 25, 495–511.

Mackay, J.R., 1998. Pingo growth and collapse, Tuktoyaktuk Peninsula Area, Western Arctic Coast, Canada: a long-term field study. Géographie Physique et Quaternaire 52, 271–323.

Mackay, J.R., Burn, C.R., 2011. A century (1910–2008) of change in a collapsing pingo, Parry Peninsula, western Arctic coast, Canada. Permafrost and Periglacial Process Online First. doi:10.1002/ppp. 723.

Marsh, P., Russell, M., Pohl, S., Haywood, H., Onclin, C., 2009. Changes in thaw lake drainage in the Western Canadian Arctic from 1950 to 2000. Hydrological Processes 23, 145–158.

Müller, F., 1959. Observations on pingos—detailed studies in East Greenland and the Canadian Arctic Beobachtungen über Pingos, Detailuntersuchungen in Ostgrönland und in der Kanadischen Arktis. Meddelelser om Grønland 153 (3) 127 p.

Muller, S.W., 1945. Permafrost or Permanently Frozen Ground and Related Engineering Problems. Military Intelligence Division, Office, Chief of Engineers, U.S. Army, Washington, D.C (second printing with corrections), 231 p.

Nelson, F.E., Outcalt, S.I., Goodwin, C.W., Hinkel, K.M., 1985. Diurnal thermal regime in a peat-covered palsa, Toolik Lake, Alaska. Arctic 38, 310–315.

Nelson, F.E., Hinkel, K.M., Outcalt, S.I., 1992. Palsa-scale frost mounds. Periglacial Geomorphology: Proceedings of the 22nd Annual Binghamton Symposium in Geomorphology, pp. 305–325.

Nolan, M., Prokein, P., 2003. Evaluation of a new DEM of the Putuligayuk Watershed for Arctic hydrological applications. Proceedings of the 8th International Permafrost Conference, Zurich, Switzerland, July 2003.

Outcalt, S.I., Nelson, F.E., Hinkel, K.M., Martin, G.D., 1986. Hydrostatic-system palsas at Toolik lake, Alaska: field observations and simulation. Earth Surface Process Landforms 11, 79–94.

Papp, K.A., Prakash, A., Collett, T.S., 2005. Integrated analysis of permafrost features, gas seeps, gas hydrate and geologica structures southwest of Prudhoe Bay, Alaska. American Geophysical Union, Fall Meeting 2005. abstract #C11A-1061.

Pissart, A., 1967. Les pingos de l'ile Prince Patrick (76°N–120°W). Geographical branch, mines and technical surveys, Ottawa. Geographical Bulletin 9, 189–217.

Pissart, A., 2002. Palsas, lithalsas and remnant of these periglacial mounds: a progress report. Progress Physics Geography 26, 605–621.

Pollard, W.H., van Everdingen, R.O., 1992. Formation of seasonal ice bodies. In: Dixon, J.C., Abrahams, A.D. (Eds.), Periglacial Geomorphology. Wiley, New York, pp. 281–304.
Porsild, A.E., 1929. Reindeer Grazing in Northwest Canada. Canada Dept. Int., Northwest Territories and Yukon Branch, Ottowa. 46 p.
Porsild, A.E., 1938. Earth mounds in unglaciated Arctic northwestern America. Geographical Review 28 (1), 46–58.
Seppala, M., 1986. The origin of palsas. Geografiska Annaler 68A, 141–147.
Shumskii, P.A., Vtyurin, B.I., 1966. Underground ice. First International Conference on Permafrost, Lafayette, Indiana, 1963. National Academy of Science, National Research Council, Washington, D.C, pp. 108–113. Publication 1287.
Skirvin, S., Casavant, R., Burr, D., 2008. Subsurface tectonics and pingos of northern Alsaka. American Geophysical Union, Fall Meeting 2008. abstract #P33B-1447.
Soare, R.J., Burr, D.M., Wan Bun Tseung, J.M., 2005. Possible pingos and a periglacial landscape in northwest Utopia Planitia. Icarus 174, 373–382.
Stager, J.K., 1956. Progress report on the analysis of the characteristics and distribution of pingos east of the Mackenzie Delta. Canadian Geographic 7, 13–20.
Tsuyuzaki, S., Sawada, Y., Kushida, K., Fukuda, M., 2008. A preliminary report on the vegetation zonation of palsas in the Arctic National Wildlife Refuge, northern Alaska, USA. Ecology Research 23, 787–793.
Multi-language Glossary of Permafrost and Related Ground-ice Terms. In: van Everdingen, R. (Ed.), National Snow and Ice Data Center/World Data Center for Glaciology, Boulder. Revised in May 2005.
Vtyurin, B.I., 1975. Underground ice in the U.S.S.R. (in Russian). Nauka, Moskow. 212.
Walker, D.A., Walker, M.D., Everett, K.R., Webber, P.J., 1985. Pingos of the Prudhoe Bay Region. Alaska. Arctic Alpine Research 17, 321–336.
Wang, B., French, H.M., 1995. Permafrost on the Tibet Plateau, China. Quaternary Science Reviews 14, 255–274.
Williams, J.R., Yeend, W.E., Carter, L.D., Hamilton, T.D., 1977. Preliminary surficial deposits map of National Petroleum Reserve-Alaska. U.S. Geological Survey, Open-File Report, pp. 77–868.
Worsley, P., Gurney, S.D., Collins, E.E., 1995. Late holocene 'mineral palsas' and associated vegetation patterns: a case study from Lac Hendry, Northern Quebec, Canada and significance for european pleistocene thermokarst. Quaternary Science Reviews 14, 179–192.
Worsley, P., Gurney, S.D., 1996. Geomorphology and hydrogeological significance of the Holocene pingos in the Karup Valley area, Traill Island, northern east Greenland. Journal of Quaternary Science 11, 249–262.
Wu, Z., Barosh, P.J., Hu, D., Wu, Z., Peisheng, Y., Qisheng, L., Chunjing, Z., 2005. Migrating pingos in the permafrost region of the Tibetan Plateau, China and their hazard along the Golmud-Lhasa railway. Engineering Geology 79, 267–287.
Yoshikawa, K., Harada, K., 1995. Observations on nearshore pingo growth, Adventdalen, Spitsbergen. Permafrost and Periglacial Process 6, 361–372.